New Journal of Physics
The open access journal at the forefront of physics

Deutsche Physikalische Gesellschaft DPG
IOP Institute of Physics

Published in partnership with: Deutsche Physikalische Gesellschaft and the Institute of Physics

OPEN ACCESS

RECEIVED
29 September 2017

REVISED
25 January 2018

ACCEPTED FOR PUBLICATION
19 February 2018

PUBLISHED
28 March 2018

PAPER

Enhanced laser-energy coupling to dense plasmas driven by recirculating electron currents

R J Gray[1], R Wilson[1], M King[1], S D R Williamson[1], R J Dance[1], C Armstrong[1,2], C Brabetz[3], F Wagner[3], B Zielbauer[3], V Bagnoud[3], D Neely[1,2] and P McKenna[1]

[1] SUPA Department of Physics, University of Strathclyde, Glasgow G4 0NG, United Kingdom
[2] Central Laser Facility, STFC Rutherford Appleton Laboratory, Oxfordshire OX11 0QX, United Kingdom
[3] Plasma Physics Department, GSI Helmholtzzentrum fuer Schwerionenforschung GmbH, D-64291 Darmstadt, Germany

E-mail: paul.mckenna@strath.ac.uk

Keywords: laser–plasma interactions, laser absorption, relativistic plasma

Abstract

The absorption of laser energy and dynamics of energetic electrons in dense plasma is fundamental to a range of intense laser-driven particle and radiation generation mechanisms. We measure the total reflected and scattered laser energy as a function of intensity, distinguishing between the influence of pulse energy and focal spot size on total energy absorption, in the interaction with thin foils. We confirm a previously published scaling of absorption with intensity by variation of laser pulse energy, but find a slower scaling when changing the focal spot size. 2D particle-in-cell simulations show that the measured differences arise due to energetic electrons recirculating within the target and undergoing multiple interactions with the laser pulse, which enhances absorption in the case of large focal spots. This effect is also shown to be dependent on the laser pulse duration, the target thickness and the electron beam divergence. The parameter space over which this absorption enhancement occurs is explored via an analytical model. The results impact our understanding of the fundamental physics of laser energy absorption in solids and thus the development of particle and radiation sources driven by intense laser–solid interactions.

Introduction

Laser energy absorption by electrons is central to high intensity laser–plasma interaction physics. It strongly influences the optical properties of the plasma [1, 2] and the characteristics of beams of high energy photons [3, 4] and ions [5, 6] produced. Given that the energy coupling to electrons is highly sensitive to a number of interrelated and evolving laser and plasma parameters, absorption remains one of the most challenging areas of the field to understand. Addressing this challenge is essential for the many applications which require efficient energy transfer to particles and radiation, such as advanced ignition schemes for inertial confinement fusion [7, 8] and isochoric heating of matter [9].

In the case of dense plasma, the dominant laser energy coupling mechanisms, such as $\mathbf{J} \times \mathbf{B}$ acceleration [10], vacuum heating [11] and resonance absorption [12], are sensitive to parameters including the laser polarisation and intensity, its incidence angle onto target and the density scale length of the target plasma [13–15]. In addition, the occurrence of multiple absorption mechanisms and transitions between mechanisms as the laser–plasma interaction evolves, make it difficult to investigate the coupling dynamics experimentally. In the absence of experimental techniques to resolve the various coupling processes occurring on ultrashort time-scales, we can progress our understanding of the overall absorption physics by determining the *total* laser absorption from measurements of the reflected and scattered laser light [16, 17], and its dependency on laser and plasma parameters. The resulting, essentially empirical, insight feeds into the future design of experiments and is ultimately essential for the verification of theoretical and numerical models of absorption physics.

To date, there are few experimental measurements of total absorption in the relativistic laser–dense plasma interaction regime. Results reported in Ping *et al* [18], for 0.8 μm wavelength laser pulses with duration equal to

150 fs and energy between 0.02 and 20 J, demonstrate an intensity dependent scaling of laser absorption which extends beyond 90% at $\sim 2 \times 10^{20}$ W cm^{-2}. These results were utilised to develop an empirical scaling law [19] and to develop a theoretical model which identifies upper and lower bounds on laser-coupling for a given laser intensity [20]. Whilst this demonstrates that absorption depends strongly on laser intensity by variation of pulse energy, the influence of focal spot size and pulse duration on total energy absorption in the relativistic regime is not well characterised. Changes to the flux and temperature of the electrons inferred from measurements of laser-driven proton acceleration and x-ray generation indicate that there are more complex coupling dynamics at work when the focal spot size is varied and this merits further investigation [21–23].

In this article, we report on the first measurements of total absorption scaling as a function of laser intensity in which the pulse energy and focal spot size are separately varied, for the case of relativistic laser–foil interactions. We demonstrate that the scaling of the absorption with intensity by variation of focal spot size is significantly slower than by variation of laser pulse energy. Particle-in-cell (PIC) simulations reveal that enhanced absorption observed with relatively large focal spot sizes is a consequence of additional heating of the relativistic electrons which recirculate within the target between the sheath fields formed on the surfaces [24]. Using a simple analytical model, we explore the parameter space for which this effect occurs and show that it is a function not only of the focal spot size but also the laser-pulse duration, target thickness and the electron spectral and divergence distributions. The results highlight the importance of considering changes to absorption caused by the recirculating population of relativistic electrons in experiment design and ultimately in the development of laser-driven particle and radiation sources.

Methodology

The experiment was performed using the high power PHELIX laser at the GSI laboratory near Darmstadt. Linearly polarised pulses with duration, τ_L, equal to (700 $\pm$ 100) fs (full width at half maximum, FWHM), with energy, E_L, varied between 4 and 180 J and a central wavelength of 1.053 μm, were incident at 0° (i.e. along the target normal axis) onto aluminium foil targets with thickness, l, equal to 6 and 20 μm. The laser intensity contrast was 10^{-12} at 1 ns and 10^{-4} at 10 ps, prior to the peak of the pulse [25]. The laser energy was changed by the rotation of a calibrated wave plate between two crossed polarisers between the front end and preamplifier sections. The energy range from 10 to 200 J can be selected without any additional change to the laser or beamline configuration, and consequently the contrast does not change significantly over that range. This was verified via test shots with extremely thin foil targets at full power and the use of a third-order scanning autocorrelator at low energies. An $f/1.5$ off-axis parabola was used to focus the laser pulse to a focal spot diameter, ϕ_L, which was varied in the range 4–270 μm (FWHM) by movement of the parabola toward a fixed target position. By separately varying E_L and ϕ_L, we investigate laser absorption over the intensity range $I_L = 10^{17}$–10^{20} W cm^{-2}.

We developed and deployed two novel diagnostics which operate simultaneously to measure the total laser absorption. As shown in figure 1, a custom 180 mm diameter integrating (Ulbricht) sphere was developed to make measurements of the total unabsorbed laser pulse energy, from which the absorbed fraction is determined [26]. The sphere was divided into two hemispheres to enable access for a focal spot and target alignment camera prior to laser irradiation of the target foil positioned at the centre of the sphere. After the target was aligned the two hemispheres were moved together forming a tight seal at the interface. A 70 mm diameter aperture at the equator of the sphere accommodates the full focusing laser cone and a 30 mm diameter aperture at the bottom pole enables the target mounting and positioning. Two small 2 mm diameter apertures, 50° above the equator (60° anticlockwise along the equator from laser axis) and 45° below the equator (120° clockwise along the equator from laser axis), were used for multimode optical fibre connections. The other ends of the optical fibres were connected to Ocean Optics (Maya2000Pro) and Andor Shamrock (303i) optical spectrometers. The response of the sphere was calibrated by first measuring the energy throughput of the laser system, including all optics up to the sphere entrance, using a calibrated large diameter calorimeter. The sphere response was characterised by directly irradiating the sphere walls with the laser pulse at relatively low energy levels (up to a maximum of 1 J). For full power laser pulses the fibre optic cables were filtered using well-characterised neutral density filters prior to the fibre terminal to avoid the possibility of optical damage being induced inside the fibre. The absolute energy of the scattered light in the sphere was then calculated by scaling the measured signal by a factor of the neutral density response. The unabsorbed component of the laser pulse was measured by integrating around the central laser wavelength peak by $\pm$40 nm (the range over which the spectrum decreases to the background level). At all energies the spectrometers were filtered such that only the 1st harmonic could be observed. In order to measure the backscattered and specularly reflected light from the target, which escapes the sphere and is collected by the parabola, a scatter screen was placed behind the final turning mirror before the parabola (see figure 1(a)). The backscattered light was imaged using a custom dual wavelength imaging system,

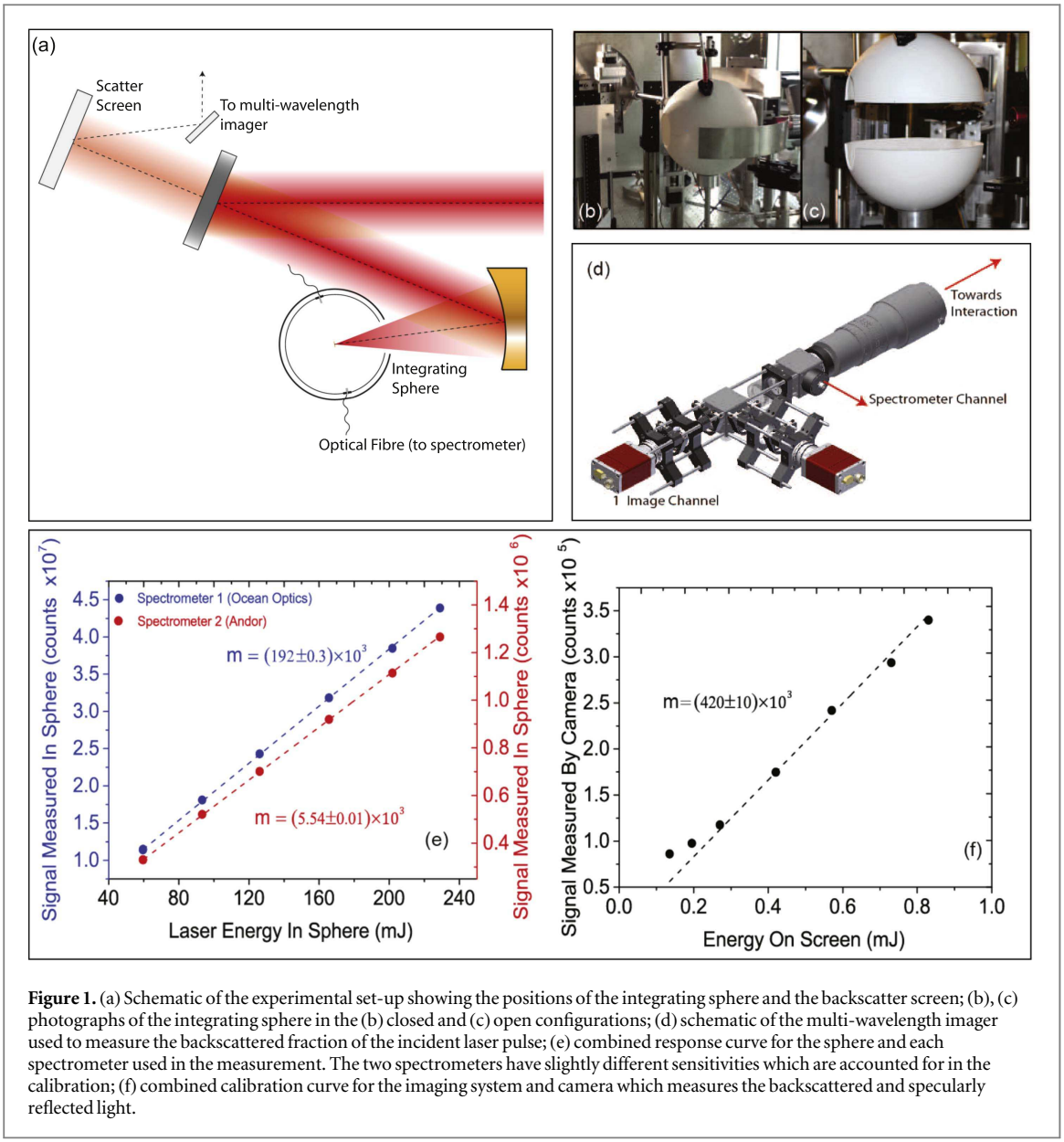

Figure 1. (a) Schematic of the experimental set-up showing the positions of the integrating sphere and the backscatter screen; (b), (c) photographs of the integrating sphere in the (b) closed and (c) open configurations; (d) schematic of the multi-wavelength imager used to measure the backscattered fraction of the incident laser pulse; (e) combined response curve for the sphere and each spectrometer used in the measurement. The two spectrometers have slightly different sensitivities which are accounted for in the calibration; (f) combined calibration curve for the imaging system and camera which measures the backscattered and specularly reflected light.

as shown in figure 1(d). An absolute calibration for the energy response of the imager was made by directly irradiating the scatter screen with light split from the incoming laser beam. A calibrated 50:50 beam-splitter was used, with one half directed onto a calorimeter and the other onto the scatter screen, thereby enabling a direct calibration of the imager response for laser pulse energy. These calibrations are shown in figures 1(e) and (f).

Measurements of laser absorption

We investigate the scaling of absorption with intensity in a similar range as the detailed investigation reported in Ping *et al* [18] (for otherwise different laser pulse parameters) and then extend our measurements to include variation of focal spot size. Specifically, we measured the change in absorption as a function of intensity by varying E_L whilst keeping ϕ_L constant (at best focus; $\phi_L = 4\ \mu$m). The results are shown in figure 2 as blue triangles for $l = 20\ \mu$m and as black squares for $l = 6\ \mu$m targets. We also plot the empirical model presented in [19] and a fit to our data with the same form:

$$f_{\mathrm{abs}} = (I_L \lambda^2 / A)^P, \tag{1}$$

where f_{abs} is the absorption fraction, $I_L\lambda^2$ is the irradiance in units of W cm^{-2} μm^2, P is a fitting parameter and $A = 3.37 \times 10^{20}$ W cm^{-2} μm^2 (from Davies [19]).

We find that our measurements are in good agreement with the predictions of the Davies model, and thus by extension the measurements reported in Ping *et al* [18] (upon which that model was based). This is despite the different laser pulse duration and other parameters explored, as detailed above. We note that for significantly

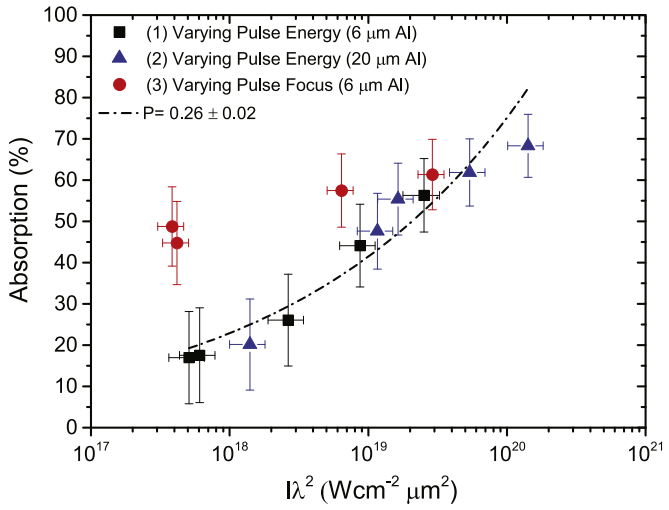

Figure 2. Measured total laser energy absorption as a function of irradiance. The black square and blue triangular data points are measurements made when the intensity is changed by varying E_L for $l = 6$ μm and $l = 20$ μm, respectively. The dot–dash line is a fit to this data using the empirical model presented in [19] and shown in equation (1), with the parameters $P = 0.26$ and $A = 3.37 \times 10^{20}$ W cm^{-2} μm^2. The red circular data points are measurements made by varying ϕ_L for constant E_L.

thinner targets (sub-micron), which may become subject to hole-boring due to the laser radiation pressure or expand to the point that relativistic self-induced transparency occurs during the interaction, a different scaling with intensity is expected due to a transition from surface-dominated to volumetric interaction processes (see for example [27–30]).

Our measurements show good agreement, in terms of scaling with I_L, with previously published values for which ϕ_L is fixed (at a few microns) and E_L varied. Published experimental measurements of the intensity scaling of the maximum energy of laser-accelerated protons and flux of x-rays suggests a different scaling when the intensity is varied by changing the laser focal spot size [21, 23, 31, 32]. We extend our direct measurements of total energy absorption to investigate this. The red circle data points in figure 2 are the measured absorption values by varying ϕ_L, for fixed E_L. Firstly, it is clear that this scaling is considerably slower than for the case of varying E_L. Secondly, we note that for $I_L \sim 5 \times 10^{17}$ W cm^{-2} there is a factor ~3 higher total absorption when using a higher energy and large focal spot. The enhanced case has considerably more energy in the pulse (157 J compared to 4 J) and a considerably larger focal spot 270 μm compared to 4 μm.

PIC simulations of laser-energy coupling

We performed simulations using the fully relativistic PIC code EPOCH (in 2D) to investigate changes to the underlying absorption physics arising from variation of ϕ_L. The laser light was linearly polarised and delivered in a $\tau_L = 550$ fs (FWHM) Gaussian pulse (a $\tau_L = 30$ fs case is considered later). The target was Al^{11+} with an initial, neutralizing electron density equal to $30n_c$ (where n_c is the critical density; the density at which the plasma frequency is equal to the laser frequency) and thickness varied between 6 and 50 μm. The initial electron and ion temperatures were 10 keV and 40 eV, respectively. A box size of up to 84 μm $\times$ 140 μm was used, with 12600 $\times$ 11520 cells and 10 particles per cell.

In the first instance, we selected I_L and ϕ_L values to be the same as two of the experimental data points, to enable comparison. We consider a peak intensity of ~1×10^{19} W cm^{-2}, with $\phi_L = 50$ μm and $\phi_L = 4$ μm. Since it is not possible to deconvolve the incoming and reflected laser fields from the fields associated with the expanding electron population, the energy content and temperature of the electrons is considered in lieu of an absorption measure. Example electron spectra at a time $t = 334$ fs after the peak of the pulse interaction (i.e. the time prior to the fastest electrons leaving the simulation box) are shown in figure 3(a). This exhibits behaviour consistent with the experiment, namely that the larger spot case results in a higher total energy of relativistic electrons compared to the smaller spot case. The inset of figure 3(a) shows the normalised energy difference in the total electron energy above the initial thermal energy for $\phi_L = 50$ μm compared to $\phi_L = 4$ μm ($\epsilon_{50\mu m}$ and $\epsilon_{4\mu m}$, respectively) as a function of time. The energy gain increases as the intensity increases on the rising edge of the laser pulse and saturates towards the peak of the laser pulse interaction. The gain primarily comes from a non-uniform heating of electrons at the higher end of the spectrum, which changes the temperature of the high energy electrons. This result cannot be accounted for by established electron temperature scaling laws (for

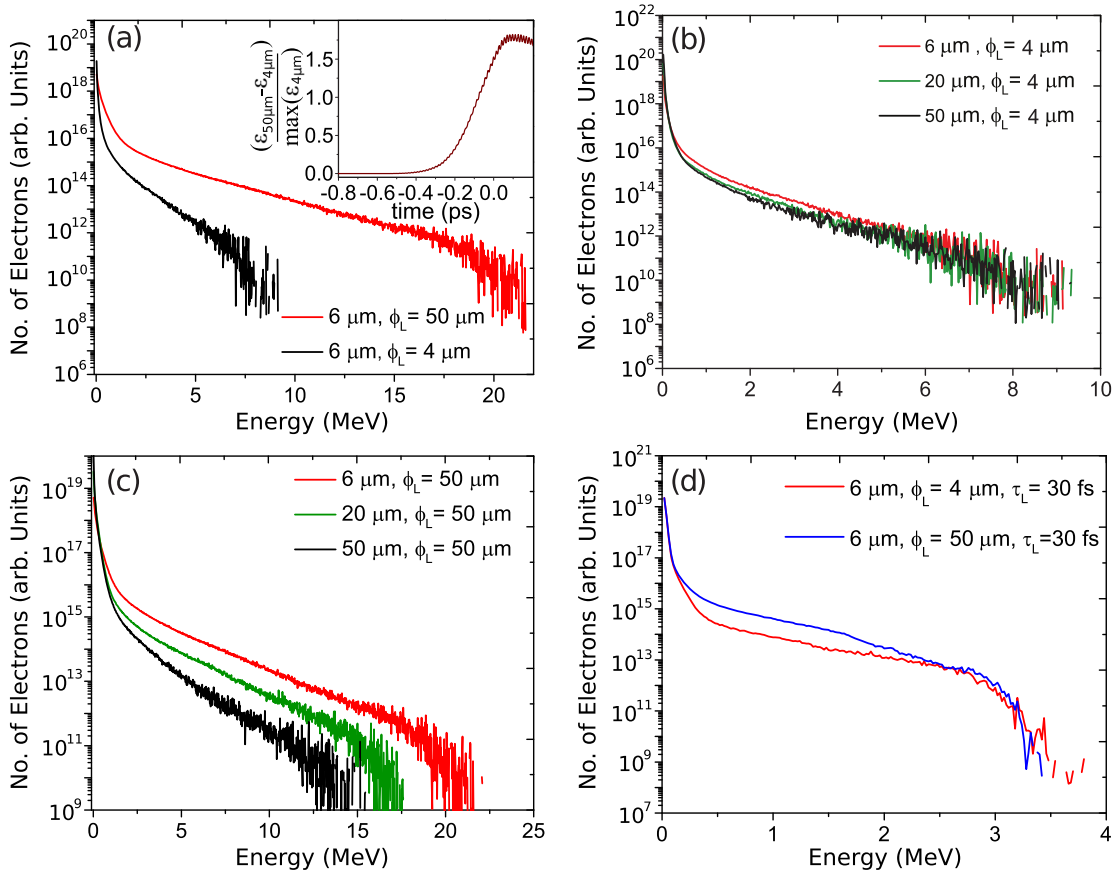

Figure 3. Electron energy spectra for: (a) focal spot sizes $\phi_L = 4$ μm and $\phi_L = 50$ μm, for fixed $l = 6$ μm and $\tau_L = 550$ fs; (b) variation in target thickness from $l = 6$–50 μm, for fixed $\phi_L = 4$ μm and $\tau_L = 550$ fs; (c) variation in target thickness from $l = 6$–50 μm, for fixed $\phi_L = 50$ μm and $\tau_L = 550$ fs; (d) focal spot sizes $\phi_L = 4$ μm and $\phi_L = 50$ μm, for fixed $l = 6$ μm and $\tau_L = 30$ fs. The inset in (a) shows the total energy difference as a function of time (for electrons above the initial electron thermal energy) between the $\phi_L = 4$ μm and $\phi_L = 50$ μm cases, normalised to the energy for $\phi_L = 4$ μm (for fixed $l = 6$ μm and $\tau_L = 550$ fs).

example, those presented in [33, 34]) or the empirical scaling of Davies [19] discussed earlier, because I_L is constant.

In order to establish if this is a surface interaction effect (e.g. changes in the absorption mechanism or deformation of the critical density surface) or if it arises due to volumetric effects, we investigated the effect of changing l for both $\phi_L = 50$ μm and $\phi_L = 4$ μm. The target thicknesses investigated were $l = 6$, 20 and 50 μm. The results of these simulations are shown in figures 3(b) and (c), again by extracting the electron spectrum sampled 334 fs after the peak of the pulse. For $\phi_L = 4$ μm the electron spectrum and temperature are essentially independent of target thickness (figure 3(b)). By contrast, for the $\phi_L = 50$ μm case (figure 3(c)), there is a significant change in the electron spectra as l is changed, with the thinnest targets resulting in the highest temperature and electron energies. For large ϕ_L, decreasing l leads to significant changes in the measured electron spectra. For small l, increasing ϕ_L also leads to significant changes in the spectra for constant I_L. This change (and the correlated change in the total absorption) therefore cannot be a purely surface, field driven, effect and must be related to the relativistic electron dynamics within the target bulk.

Mackinnon *et al* [35] shows via PIC simulations that the recirculation of relativistic electrons between the sheath fields [24] which build up on the surfaces can enhance the overall electron density and temperature at the rear and thereby enhance the energy of sheath-accelerated protons. Here, we propose that this recirculating electron population is in fact extracting additional energy from the laser pulse upon returning to the front surface, resulting in a higher overall laser-to-electron coupling efficiency. We test this hypothesis by reducing τ_L such that an electron close to the average energy of the spectrum ($\approx$5 MeV) could only make one pass within the target during the pulse duration and therefore gain no (or limited) additional energy from this recirculating process. As shown in figure 3(d), we measure essentially no difference in the electron spectra between the two focal spot sizes. This shows that the recirculation of relativistic electrons within the target is playing an important role in the laser-energy coupling dynamics in the interaction.

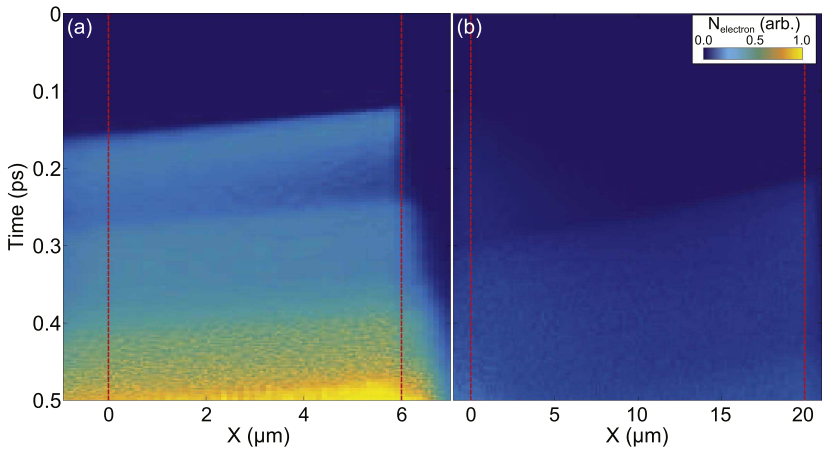

Figure 4. Temporal evolution of electron density along the laser propagation axis, for electrons with energy greater than 150 keV (to avoid sampling the background electron population) and travelling in the negative X direction (i.e. toward the laser) for $\phi_L = 50$ μm and (a) $l = 6$ μm and (b) $l = 20$ μm. The dashed red lines show the initial boundaries of the target, where $X = 0$ corresponds to the front surface.

It is difficult to directly observe the temporal dynamics of this change in the simulations after a large number of passes, given that there is a population of electrons constantly being injected while the pulse is present, in addition to the recirculating population. Since there is a large range of electron energies, after a certain distance or a number of passes through the target, the two populations become spatially indistinct. However, in the early stages of the interaction it is possible to observe the recirculating population and the additional energy gain at the front surface. This is shown in figure 4 as a time-space map of the density of electrons with energy greater than 150 keV and propagating counter to the incoming laser pulse. While the energy gain and its dependence on the number of round-trips (given a sufficiently large spot size, pulse length and electron energy) is clear from the simulations, the precise mechanism of the energy exchange is more difficult to extract. The process appears similar to that proposed in Krygier *et al* [36], where electrons leave the target propagating toward the laser pulse and are turned around by a loop magnetic field, extracting additional energy from the laser pulse via direct laser acceleration (DLA) [37]. That process typically takes place in a long density scale length plasma. For a short density scale lengths, the recirculating electrons are reflected by the sheath fields building up on the target front and rear surfaces and extract additional energy during each interaction with the laser field at the target front.

A geometric model of recirculation-enhanced absorption

These results highlight that laser intensity alone is not sufficient to predict changes in the absorption or the internal electron spectrum. Whereas I_L can be changed by varying E_L, τ_L or ϕ_L, the coupling dynamics can be radically different depending on which parameter is changed. There is a multi-dimensional parameter space in which the recirculation-enhanced absorption can occur. In order for additional energy to be extracted from the laser pulse the recirculation time (i.e. the transit time for a round trip) must be shorter than τ_L and the divergence angle of the electrons must be small enough that a sufficient number of electrons remain within the focal spot region upon their return to the front surface. The recirculation time and degree to which electrons stay within the region of the focal spot is also affected by the target thickness.

To explore this multi-dimensional parameter space in a tractable way, we construct an analytical model based purely on a ballistic (i.e not affected by self-generated fields or scattering within the target) approach to electron transport and recirculation, whereby an electron will gain a constant fraction of its initial energy upon re-interacting with the laser at the target front surface. Electron energies above 1 MeV are considered and therefore the effect of collisions is ignored, given that the distance travelled by the electron during pulse duration is small compared to the stopping range. The number of passes an electron will make during time τ_L can be shown to be

$$n_\tau = \frac{\nu_e \tau_L \cos(\theta_{\mathrm{div}})}{2l}, \tag{2}$$

where ν_e is the relativistically corrected electron velocity and θ_{div} is the angle of divergence of the electron trajectory with respect to the central axis. For a given θ_{div} it is also possible to show that the number of passes an electron will make before it leaves the laser focal spot region is

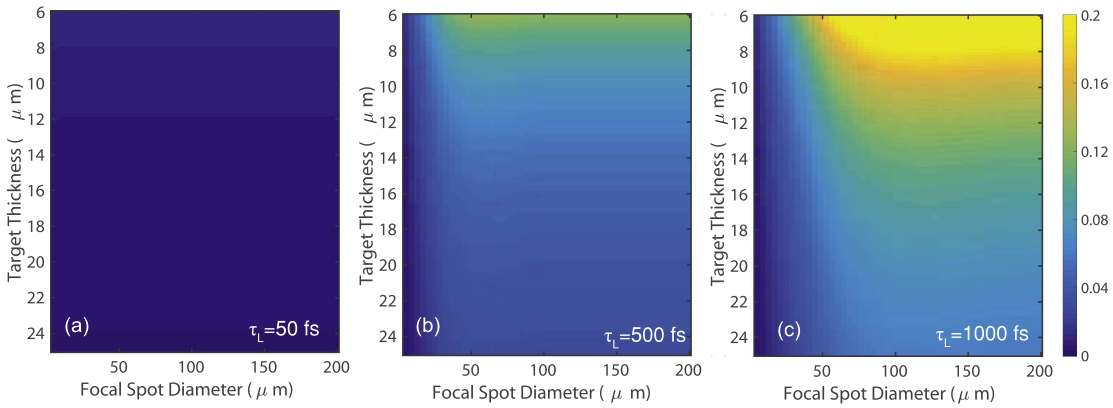

Figure 5. l–ϕ_L parameter space plots. The colour maps corresponds to the difference in total energy between the input and output spectra for τ_L equal to: (a) 50 fs; (b) 500 fs; (c) 1000 fs.

$$n_{\text{spot}} = \frac{\phi_L}{2l\tan(\theta_{\text{div}})}. \tag{3}$$

If we take the energy gained, E_{gain}, by an electron of energy E_e from the laser to be a constant fraction α of the energy, then it can be shown that the overall energy gained via recirculation will be the minimum of n_τ or n_{spot}. In other words, either the electron will gain energy until it leaves the region of the focal spot (due to its trajectory) or until the laser pulse switches off. This can be expressed as

$$E_{\text{gain}} = \frac{1}{2}(n_{\text{spot}} + n_\tau - |n_{\text{spot}} - n_\tau|)\alpha E_e. \tag{4}$$

There is of course not simply a single electron energy or divergence angle, but in fact a distribution of both. We take then $N(E_e) = N_0 e^{(-E_e/kT_e)}$ as the energy spectrum of the electron population, where T_e is the electron temperature and N_0 is the initial electron number. The energy dependent divergence angle can be calculated using the formula of Moore *et al* [38]. This gives $\theta_{\text{div}}(E_e) = \tan^{-1}(\bar{\theta}\sqrt{2/(\gamma - 1)})$, where $\bar{\theta}$ is the average divergence angle.

Using this model, the total energy gained over the spectrum due to recirculation as a function of ϕ_L and l can be examined. In figures 5(a)–(c) this parameter is plotted for l in the range 6–25 μm and ϕ_L in the range 4–200 μm, for τ_L equal to 50, 500 and 1000 fs. The total energy gain is normalised to the total energy of the input spectrum. It can be seen that for τ_L of the order of the electron transit time (i.e tens of femtoseconds) there is no additional energy gain, because the recirculating electron population does not re-interact with the laser pulse a large number of times. For longer pulse durations, as in figures 5(b) and (c), there is significant energy gain for $l < 20$ μm, but only when ϕ_L is greater than ~50 μm. The total energy gain is principally as a result of an increase in the hot tail of the spectrum, as observed in the simulations. This occurs because the highest energy electrons have the smallest divergence in the distribution and thus shortest recirculation time, and therefore interact more times the laser pulse. The higher divergence of the lower energy electrons means they move out of the region of the focal spot in a fewer number of passes and also return to the front surface a fewer number of times.

It is important to note that the range of l and τ_L for which absorption enhancement occurs is highly dependent on the choice of energy spectrum and divergence-energy functions, as well as the value of the gain coefficient α. Furthermore, the temporal evolution of the forward going electron population, as a result of the temporal evolution of the laser heating at the front surface, is not considered. Instead, we are assuming that a high energy electron population exists and allow this population to freely recirculate. Also, the population of relativistic electrons which escape the target (although often only on the order of a few percent) is not included in the model. These complexities, especially in regard to the self-consistent dynamics of the laser-injected and recirculating populations, quickly make this a complex problem to solve analytically. To that end, this simple model should be seen not as a calculation of the overall change in absorption, but illustrative of the parameter space in which recirculation-enhanced absorption is relevant.

Summary

In summary, these results demonstrate the significance of laser focal spot size in the absorption of energy into thin foils in the relativistic laser–plasma interaction regime. Complementary diagnostic techniques have been applied to determine the total energy absorption via calibrated measurements of the total laser energy specularly

reflected and scattered from the target foil. Good agreement is found with previously published results [18] of absorption scaling with laser intensity when varying the pulse energy. However, a slower scaling is measured when varying the focal spot size for a fixed laser energy, which is consistent with the picture emerging from investigations of secondary particle and radiation source properties as a function of focal spot size. PIC simulation results show that this slower absorption scaling with intensity is driven by additional heating of the relativistic electron population which recirculates within the foil between the sheath fields formed on the surfaces. This occurs when the focal spot size and pulse duration are sufficiently large and the electron beam divergence is sufficiently small to enable the recirculating population to interact multiple times with the laser field. The effect is diminished or does not occur in tight focal spot geometries or for femtosecond-scale laser pulse durations (with micron-thick targets).

The results are not only of fundamental interest, but also impact on the optimisation of laser energy coupling in relativistic laser–foil interactions and therefore influence the development of the laser-driven ion acceleration, high harmonic generation, x-ray production and other sources involving foil targets. They show that the method of varying the laser intensity (i.e. by variation of pulse duration, energy or focal spot size) can significantly change the overall energy coupling into the plasma, and by extension key properties of the secondary beams of particles and radiation produced.

Acknowledgments

We acknowledge the support of the PHELIX laser group and the use of the ARCHIE-WeST and ARCHER high performance computers. The work was supported by EPSRC (grant numbers EP/J003832/1, EP/R006202/1, EP/M018091/1, EP/K022415/1 and EP/L000237/1), STFC (Grant No. ST/K502340/1) and the European Union Horizon 2020 research and innovation program (Grant Agreement No.654148 Laserlab-Europe). EPOCH was developed under EPSRC Grant No. EP/G054940/1. Data associated with research published in this paper can be accessed at: https://doi.org/10.15129/16b2e4c8-e1ae-4673-b7d5-93898ba578ad.

ORCID iDs

P McKenna https://orcid.org/0000-0001-8061-7091

References

[1] Borghesi M *et al* 1997 *Phys. Rev. Lett.* **78** 879–82
[2] Bin J H *et al* 2015 *Phys. Rev. Lett.* **115** 064801
[3] Norreys P A *et al* 1999 *Phys. Plasmas* **6** 2150–6
[4] Cipiccia S *et al* 2011 *Nat. Phys.* **7** 867–71
[5] Snavely R A *et al* 2000 *Phys. Rev. Lett.* **85** 2945–8
[6] Macchi A, Borghesi M and Passoni M 2013 *Rev. Mod. Phys.* **85** 751–93
[7] Tabak M *et al* 1994 *Phys. Plasmas* **1** 1626–34
[8] Roth M *et al* 2001 *Phys. Rev. Lett.* **86** 436
[9] Patel P K *et al* 2003 *Phys. Rev. Lett.* **91** 125004
[10] Kruer W L and Estabrook K 1985 *Phys. Fluids* **28** 430–2
[11] Brunel F 1987 *Phys. Rev. Lett.* **59** 52–5
[12] Ginzburg V L 1964 *The Propagation of Electromagnetic Waves in Plasmas* (Oxford: Pergamon)
[13] Eidmann K, Rix R, Schlegel T and Whitte K 2001 *Europhys. Lett.* **55** 334
[14] Nishimura H *et al* 1981 *Phys. Rev.* A **23** 2011–9
[15] Singh P K *et al* 2015 *Sci. Rep.* **5** 17870
[16] Gumbrell E T *et al* 1998 *Phys. Plasmas* **5** 3714–21
[17] Teubner U *et al* 1996 *Phys. Rev.* E **54** 4167–7177
[18] Ping Y *et al* 2008 *Phys. Rev. Lett.* **100** 085004
[19] Davies J R 2008 *Plasma Phys. Control. Fusion* **51** 014006
[20] Levy M C *et al* 2014 *Nat. Commun.* **5** 4149
[21] Coury M *et al* 2012 *Appl. Phys. Lett.* **100** 074105
[22] Robson L *et al* 2007 *Nat. Phys.* **3** 58–62
[23] Chen L M *et al* 1998 *Phys. Plasmas* **11** 4439–45
[24] Sentoku Y, Cowan T E, Kemp A and Ruhl H 2003 *Phys. Plasmas* **10** 2009–15
[25] Bagnoud V *et al* 2016 *High Power Laser Sci. Eng.* **4** e39
[26] Buckley H 1921 *J. Inst. Electr. Eng.* **59** 143–52
[27] Gray R J *et al* 2014 *New. J. Phys.* **16** 093027
[28] Gonzalez-Izquierdo B *et al* 2016 *Nat. Phys.* **12** 505–12
[29] Gonzalez-Izquierdo B *et al* 2016 *Nat. Commun.* **7** 12891
[30] Powell H W *et al* 2015 *New J. Phys.* **17** 103033
[31] Brenner C M, McKenna P and Neely D 2014 *Plasma Phys. Control. Fusion* **56** 084003
[32] Quinn M N *et al* 2011 *Plasma Phys. Control. Fusion* **53** 025007

[33] Wilks S C, Kruer W L, Tabak M and Langdon A B 1992 *Phys. Rev. Lett.* **69** 1383–6
[34] Beg F N *et al* 1997 *Phys. Plasmas* **4** 447–57
[35] Mackinnon A J *et al* 2002 *Phys. Rev. Lett.* **88** 215006
[36] Krygier A G *et al* 2014 *Phys. Plasmas* **21** 023112
[37] Pukhov A, Sheng Z-M and Meyer-ter-Vehn J 1999 *Phys. Plasmas* **6** 2847
[38] Moore C I, Knauer J P and Meyerhofer D D 1995 *Phys Rev. Lett.* **74** 2439